PHYSICAL REVIEW B **80**, 155417 (2009)

Effect of Coulomb interactions on the optical properties of doped graphene

Adolfo G. Grushin, Belén Valenzuela, and María A. H. Vozmediano
Instituto de Ciencia de Materiales de Madrid, CSIC, Cantoblanco, E-28049 Madrid, Spain
(Received 9 July 2009; revised manuscript received 14 September 2009; published 6 October 2009)

Recent optical conductivity experiments of doped graphene in the infrared regime reveal a strong background in the energy region between the intra and interband transitions difficult to explain within conventional pictures. We propose a phenomenological model taking into account the marginal Fermi liquid nature of the quasiparticles in graphene near the neutrality point that can explain qualitatively the observed features. We also study the electronic Raman signal and suggest that it will also be anomalous.

DOI: 10.1103/PhysRevB.80.155417 PACS number(s): 81.05.Uw, 78.30.−j

I. INTRODUCTION

The role of many body corrections to the physics of graphene is at this point uncertain. While in the first transport experiments electron-electron interactions seemed not to play a major role,[1–3] more recent measurements indicate the possible importance of many body corrections to the intrinsic properties of graphene.[4–10] The electronic transport of single layer graphene is one of the most intriguing aspects that still lacks a full understanding. Unlike common Fermi liquids, graphene shows a minimal conductivity at zero frequency in the neutral suspended samples with a value of the order of the conductivity quantum, e^2/h that grows linearly with the electron density in the low-density regime.[2,11,12]

The optical properties of graphene (see Ref. 13 for a very accurate review) have been the focus of interest of recent experiments.[8–10,14] In the visible region, they allow a very precise determination of the value of the fine structure constant. The structure of graphene is similar to that of a two-dimensional two-band semiconductor. The dynamical conductivity is expected to have a characteristic shape where intraband (near zero energy) and interband (at an energy of twice the chemical potential, 2μ) transitions can be clearly identified. Recent observations in the infrared region of the spectrum,[10] reveal a substantial background of approximately 30 percent of the saturation value in the frequency range between intraband and interband transitions. The observed background remains approximately constant for several values of the chemical potential that range from 0.10 eV up to 0.30 eV. Moreover, the threshold at 2μ shows a very wide width independent of gate voltage and therefore of carrier density.

A strong background was also observed in the early times of high-T_c superconductors and prompted the marginal Fermi liquid ideas.[15] Together with the observation of the anomalous infrared optical conductivity in Ref. 10 they observe an increase of the Fermi velocity with lowering the frequency at low energies which is suggested to be due to the renormalization of the Fermi velocity from the electron-electron interactions as predicted in early works.[16,17] The measures of optical properties as a function of the frequency for varying chemical potential,[9,14] angle resolved spectroscopy (ARPES)[5,6,18] or scanning tunneling microscopy (STM)[7] are complementary probes to explore the influence of disorder and interactions on the properties of graphene. In this work, we propose that the mid infrared residual conductivity found in the experiments at finite chemical potential can be a footprint of the anomalous behavior of the electron lifetime at the Dirac point.[19] We compute the optical conductivity with a phenomenological self-energy based on the marginal Fermi liquid behavior discussed in Ref. 19 and see that it helps to understand the experiments. We predict a similar anomalous background in the electronic contribution to the Raman signal, which has not been measured yet in graphene.

II. MAIN ELECTRONIC PROPERTIES OF GRAPHENE

As it is well known by now, graphene is a two dimensional array of carbon atoms with a sp^2 coordination. An updated review of its properties can be found in Ref. 20. The strong sp^2 sigma bonds form a honeycomb lattice and the low-energy electronic structure comes from the π electrons perpendicular to the plane located at the sites of the honeycomb structure. Due to the special topology of the honeycomb lattice that has two atoms per unit cell and lacks inversion symmetry, the Fermi surface of the neutral system consists of two inequivalent Fermi points[21] and the low-energy excitations around them are described in the continuum limit by the two dimensional massless Dirac Hamiltonian.[22] The low-energy dispersion relation of the two bands around a Fermi point is

$$\epsilon(\mathbf{k}) = \pm v_F|\mathbf{k}|,$$

from where it can be seen that the density of states vanishes at the Fermi energy and the effective mass of the quasiparticles is zero. v_F is the Fermi velocity estimated to be $v_F \sim 10^6$ m/s $\sim c/300$.

The low-energy nature of the interacting system was studied with renormalization group techniques in Ref. 16. Due to the vanishing of the density of states at the Fermi energy the Coulomb interaction is unscreened and the neutral system departs from the usual Fermi liquid behavior. In particular, the inverse lifetime of the quasiparticles was found in Ref. 19 to decrease linearly with the frequency instead of the squared Fermi-liquid behavior.

III. PHENOMENOLOGOCAL MODEL FOR THE ELECTRON SELF-ENERGY

The main idea of this work is that the physics of the Dirac point influences the infrared properties of the doped system.

This assumption has some experimental support. In the photoemission analysis done in Ref. 18 it is shown that interactions deform the spectral function of doped graphene not only at the Fermi level but also at the position of the Dirac cone. In the early work,[19] it was shown that the inverse lifetime of intrinsic graphene grows linearly with energy at low energies, an infrared behavior typical of the marginal Fermi liquid.[15] The inverse lifetime of electrons in the presence of the unscreened Coulomb interaction was found to be:

$$\mathrm{Im}\,\Sigma(\omega) = \frac{1}{48}\left(\frac{\alpha}{\epsilon_0}\right)^2\left(\frac{c}{v_F}\right)^2|\omega|, \tag{1}$$

where α is the fine structure constant and ϵ_0 is the dielectric constant ($\epsilon_0=2.4$ for graphite). This result has been corroborated by recent experiments[7] that provide an estimation of the coefficient of the linear scattering rate of the order of 0.07 in a range of energies up to ~ 0.15 eV.[23]

From a linearly dependent imaginary part of the electron self-energy $\mathrm{Im}\,\Sigma(\omega)=a|\omega|$, and computing the real part by a Kramers-Kronig transformation we get the "marginal Fermi liquid" type of the electron self-energy:

$$\Sigma_{MFL}(\omega) = \frac{2a}{\pi}\left[\omega \ln\left(\frac{\omega_c}{\omega}\right) + i\frac{\pi}{2}|\omega|\right] + ib, \tag{2}$$

where we have also added a constant scattering rate. While in the physics of cuprates the electron self-energy shows a marginal Fermi liquid behavior for a large range of doping levels,[15] in the case of graphene the marginal behavior is restricted to a very small energy region around the zero doping and chemical potential. We will take this fact into account by considering the following phenomenological electron self-energy:

$$\mathrm{Im}\,\Sigma(\omega) = \begin{cases} a|\omega| + b, & |\omega| < \Lambda \\ a\Lambda + b, & |\omega| \geq \Lambda \end{cases}, \tag{3}$$

where Λ is a low energy cutoff that will be set to $\Lambda \sim 0.15$ eV. As mentioned before realistic values for the parameters a, b estimated from the experiment[7] are $a=0.07$, $b=0.01$ eV although they may vary from sample to sample.

A Kramers-Kronig transformation of Eq. (3) gives for the real part

$$\mathrm{Re}\,\Sigma(\omega) = \frac{a}{\pi}\left[\Lambda \ln\left(\frac{\Lambda+\omega}{\Lambda-\omega}\right) + \omega \ln\left(\frac{\omega^2-\Lambda^2}{\omega^2}\right)\right]. \tag{4}$$

IV. OPTICAL PROPERTIES OF THE MODEL

From the Kubo formula we can write the optical conductivity as a function of the electron spectral function $A_s(k,\omega)$ in the so-called bubble approximation that neglects the vertex corrections:[24]

$$\mathrm{Re}\,\sigma(\omega) = g_s g_v \frac{e^2 v_F^2}{4\omega}\sum_{s,s'}\int \frac{kdk}{(2\pi)^2}\cdot$$

$$\int d\epsilon [n_F(\epsilon) - n_F(\epsilon+\omega)] A_s(k,\omega) A_{s'}(k,\epsilon+\omega), \tag{5}$$

where $g_{s,v}$ are the spin and valley degeneracies, $n_F(\epsilon)=\{\exp[\beta(\epsilon-\mu)]+1\}^{-1}$ is the Fermi distribution function, and $A_s(\mathbf{k},\omega)$ is the spectral function:

$$A_s(k,\omega) = \frac{-2\,\mathrm{Im}\,\Sigma(\omega,\mathbf{k})}{[\omega - sv_F|\mathbf{k}| - \mathrm{Re}\,\Sigma(\omega,\mathbf{k})]^2 + [\mathrm{Im}\,\Sigma(\omega,\mathbf{k})]^2}. \tag{6}$$

The index $s=\pm 1$ refers to the upper (lower) part of the dispersion relation. The bubble approximation works well if the electron self-energy is not strongly k-dependent[25] as happens in our case.

Finally for systems with a very isotropic Fermi surface as it is our case the electronic contribution to the Raman signal $\mathrm{Im}\,\chi(\omega)$ can be related to the optical conductivity by the simple expression:[26]

$$\omega\,\mathrm{Re}\,\sigma(\omega) \sim \mathrm{Im}\,\chi(\omega). \tag{7}$$

V. RESULTS AND DISCUSSION

We have computed the optical conductivity at zero temperature from Eqs. (3) and (5). Figure 1 contains the main result of this work. It shows a comparison between the dynamical conductivity measured in Ref. 10 (a) and that obtained with the self-energy given by Eq. (3) (b) for the following values of the parameters: $a=0.2$, $b=0.001$ eV, and $\Lambda=0.15$ eV. In the experimental figure, it can be seen a contribution coming from de Drude peak at low energies, the interband transitions beyond 2μ and the strong background between the Drude peak and the interband transitions. It can also be appreciated that the width of the threshold of the interband transitions at 2μ is very wide and almost independent of the electronic density. In our approach, we obtain the most prominent characteristics of the experimental results as can be appreciated in Fig. 1(b).

In order to clarify the role of the Coulomb interactions encoded in parameter a of Eq. (3) versus a simple constant scattering rate b, we have shown in Fig. 2(a) a comparison of the optical conductivity computed with the self-energy Eq. (2) for parameters $a=0.2$, $b=0.001$ eV, $\Lambda=0.15$ eV, and $\mu=0.18$ eV (red solid line) and the same with only a constant scattering rate ($a=0$) (blue dashed line). For the constant scattering rate the intermediate frequency region between Drude and interband transitions is almost zero and the threshold is sharp. We have checked that the same kind of behavior of the conductivity is found using a Fermi-liquid type of self-energy which is expected to correspond to doped graphene.[27] When the linear contribution to the scattering rate is added the Drude peak becomes wider, there is a considerable background at intermediate frequencies and the threshold of the interband transitions acquires a finite width. All these characteristics are expected from a linear scattering rate since it induces a general shift of the spectral weight from lower to higher frequencies. It is worth mentioning that although we have added the cutoff Λ in expression Eq. (3) to

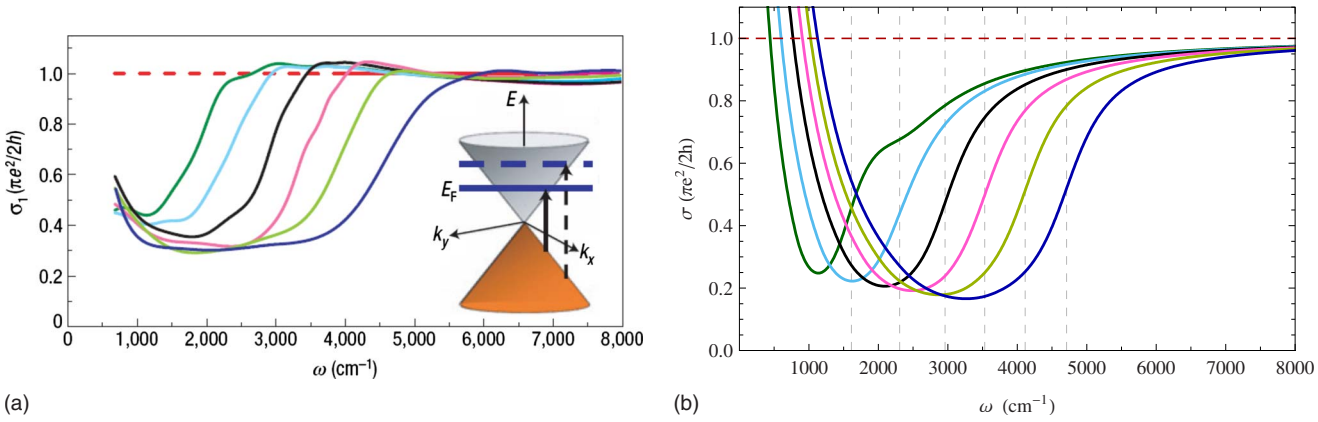

FIG. 1. (Color online) (a) Measured optical conductivity of graphene for different gate voltages (from right to left V_g=71, 54, 40, 28, 17, and 10 V). The dashed red line is the optical conductivity at zero chemical potential. This figure has been adapted by permission from Macmillan Publishers. (b) Conductivity computed with the self-energy Eq. (3) for parameters a=0.2, b=0.001 eV, Λ=0.15 eV and for the same gate voltages. The vertical dashed lines indicate the $2E_F$ threshold at each chemical potential.

restrict the marginal behavior to low frequencies, the shift of the spectral weight is quite remarkable.

The problem of the anomalous residual conductivity was studied in Refs. 28 and 29 taking into account unitary scatterers, charge impurities, and optical and acoustic phonons. They arrive to the result that to account for the observed value of the residual conductivity another mechanism effective at high energies must be included. They also obtain that optical phonons give a marginal contribution similar to Coulomb interactions for frequencies away from the Dirac point. Some types of disorder also induce a linear behavior on the scattering rate at low energies.[30]

What we see from our analysis is that including a linear imaginary part of the self-energy even for a very low-energy range stabilizes the background of the conductivity and widens the threshold of the interband transitions in a way that is almost independent of the electronic density. To get a better fit for the experimental data we have chosen a big value of the slope of the linear scattering rate "a." We must mention that besides the electronic interaction there can be other contributions to the linear scattering rate coming from disorder[30] or optical phonons.[28,29]

Figure 2(b) shows the same comparison for the electronic contribution to the Raman signal in graphene yet to be measured. Dashed blue curve refers to the case with a constant scattering rate. The electronic Raman scattering has been calculated very recently in Ref. 31. In agreement with our work, they also find a linear spectral density beyond 2μ coming from interband transitions. We obtain a Drude contribution at low energy coming from the constant scattering rate b=0.001 eV (dotted blue line). As happens in the optical conductivity there is no spectral weight in the region between intra and interband transition when only a constant scattering rate is considered. Adding the marginal like behavior however (red solid line) there is a noticeable background at intermediate frequencies and there are no sharp separations between the Drude contribution, the background and the interband transitions. The inset of Fig. 2(b) shows the variation of the Raman spectrum with the chemical potential. The values plotted are the same as in the optical conductivity. The three main characteristics, i.e.: Drude contribution, interband transitions, and background are clearly seen. For lower chemical potentials it can be seen that the Drude peak shifts to higher frequencies when increasing μ since the lin-

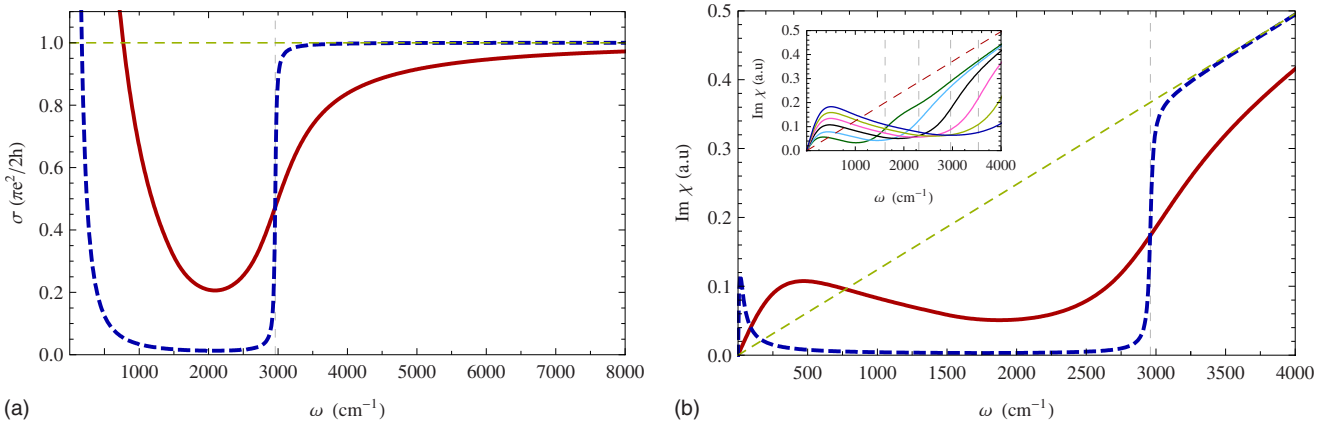

FIG. 2. (Color online) (a) Comparison of the optical conductivity computed with the self-energy Eq. (2) for parameters a=0.2, b=0.001 eV, and Λ=0.15 eV, μ=0.18 eV (red solid line) and same with a constant scattering rate only, i. e., a=0 (blue dashed line). (b) Same comparison for the Raman signal. The inset shows the evolution of the Raman signal obtained with the self-energy Eq. (3) for decreasing values of the chemical potential from top to bottom. The same color code as in the optical conductivity is used.

ear contribution dominates the physics. This behavior will also be present in the Drude contribution of the optical conductivity but such low frequencies are not accessible in optical conductivity experiments.

To summarize, we have proposed a phenomenological model that includes the linear behavior of the scattering rate at low frequencies and shown that it can explain qualitatively recent experiments in optical conductivity of graphene.[10] The linear scattering rate might have its origin on electronic interactions as discussed in this paper but optical phonons and disorder can also contribute to strengthen the marginal Fermi liquid type of behavior. In particular, we have obtained the strong background observed between the Drude peak and interband transitions and the wide width of the threshold of the interband transitions, two features that are difficult to explain using a Fermi liquid picture. We have predicted that an anomalous background will be also seen in other optical probes such as electronic Raman scattering.

ACKNOWLEDGMENTS

We acknowledge very useful conversations with Fernando de Juan and Javier Sabio. We also thank Dimitri Basov for kindly allowing us to reproduce Fig. 2(b) of Ref. 10. This research was supported by the Spanish MECD under Grants No. FIS2005-05478-C02-01 and No. FIS2008-00124.

[1] K. S. Novoselov, A. K. Geim, S. V. Morozov, D. Jiang, Y. Zhang, S. V. Dubonos, I. V. Gregorieva, and A. A. Firsov, Science **306**, 666 (2004).
[2] K. S. Novoselov, A. K. Geim, S. V. Morozov, D. Jiang, M. I. Katsnelson, I. V. Grigorieva, S. V. Dubonos, and A. A. Firsov, Nature (London) **438**, 197 (2005).
[3] Y. Zhang, Y.-W. Tan, H. L. Stormer, and P. Kim, Nature (London) **438**, 201 (2005).
[4] Z. Jiang, E. A. Henriksen, L. C. Tung, Y.-J. Wang, M. E. Schwartz, M. Y. Han, P. Kim, and H. L. Stormer, Phys. Rev. Lett. **98**, 197403 (2007).
[5] A. Bostwick, T. Ohta, T. Seyller, K. Horn, and E. Rotenberg, Nat. Phys. **3**, 36 (2007).
[6] S. Y. Zhou, D. A. Siegel, A. V. Fedorov, and A. Lanzara, Phys. Rev. B **78**, 193404 (2008).
[7] G. Li, A. Luican, and E. Y. Andrei, Phys. Rev. Lett. **102**, 176804 (2009).
[8] R. Nair, P. Blake, A. Grigorenko, K. Novoselov, T. Booth, T. Stauber, N. Peres, and A. Geim, Science **320**, 1308 (2008).
[9] K. F. Mak, M. Y. Sfeir, Y. Wu, C. H. Lui, J. A. Misewich, and T. F. Heinz, Phys. Rev. Lett. **101**, 196405 (2008).
[10] Z. Q. Li, E. A. H. Z. Jiang, Z. Ha, M. C. Martin, P. Kim, H. L. Stormer, and D. N. Basov, Nat. Phys. **4**, 532 (2008).
[11] K. S. Novoselov, E. McCann, S. V. Morozov, V. I. Falko, M. I. Katsnelson, U. Zeitler, D. Jiang, F. Schedin, and A. K. Geim, Nat. Phys. **2**, 177 (2006).
[12] M. I. Katsnelson, K. S. Novoselov, and A. K. Geim, Nat. Phys. **2**, 620 (2006).
[13] V. Gusynin, S. Sharapov, and J. Carbotte, Int. J. Mod. Phys. B **21**, 4611 (2007).
[14] A. B. Kuzmenko, E. van Heumen, F. Carbone, and D. van der Marel, Phys. Rev. Lett. **100**, 117401 (2008).
[15] C. M. Varma, P. B. Littlewood, S. Schmitt-Rink, E. Abrahams, and A. E. Ruckenstein, Phys. Rev. Lett. **63**, 1996 (1989).
[16] J. González, F. Guinea, and M. A. H. Vozmediano, Nucl. Phys. B **424**, 595 (1994).
[17] J. González, F. Guinea, and M. A. H. Vozmediano, Phys. Rev. B **59**, R2474 (1999).
[18] A. Bostwick, T. Ohta, J. L. McChesney, Seyller, K. Horn, and E. Rotenberg, Solid State Commun. **143**, 63 (2007).
[19] J. González, F. Guinea, and M. A. H. Vozmediano, Phys. Rev. Lett. **77**, 3589 (1996).
[20] A. H. Castro Neto, F. Guinea, N. M. R. Peres, K. S. Novoselov, and A. K. Geim, Rev. Mod. Phys. **81**, 109 (2009).
[21] P. R. Wallace, Phys. Rev. **71**, 622 (1947).
[22] G. W. Semenoff, Phys. Rev. Lett. **53**, 2449 (1984).
[23] We thank Eva Andrei for providing this estimation to us.
[24] G. D. Mahan, *Many-Particle Physics*, 2nd ed. (Plenum Press, New York, 1993).
[25] A. J. Millis, in *Strong Interactions in Low Dimensions*, edited by D. Baeriswyl and L. Degiorgi (Kluwer Academic, The Netherlands, 2004).
[26] B. S. Shastry and B. I. Shraiman, Phys. Rev. Lett. **65**, 1068 (1990).
[27] S. Das Sarma, E. H. Hwang, and W.-K. Tse, Phys. Rev. B **75**, 121406(R) (2007).
[28] N. M. R. Peres, T. Stauber, and A. H. Castro Neto, Europhys. Lett. **84**, 38002 (2008).
[29] T. Stauber, N. M. R. Peres, and A. H. Castro Neto, Phys. Rev. B **78**, 085418 (2008).
[30] Y. Z. T. Ando and H. Suzuura, J. Phys. Soc. Jpn. **71**, 1318 (2002).
[31] O. Kashuba and V. I. Fal'ko, arXiv:0906.5251 (unpublished).